Landes Bioscience www.landesbioscience.com

Supplemental Material to:

Sylvain Ladoire, Kariman Chaba, Isabelle Martins, Abdul Qader Sukkurwala, Sandy Adjemian, Mickaël Michaud, Vichnou Poirier-Colame, Felipe Andreiuolo, Lorenzo Galluzzi, Eileen White, Mathias Rosenfeldt, Kevin M. Ryan, Laurence Zitvogel and Guido Kroemer

Immunohistochemical detection of cytoplasmic LC3 puncta in human cancer specimens

Autophagy 2012; 8(8)
http://dx.doi.org/10.4161/auto.20353

www.landesbioscience.com/journals/autophagy/article/20353

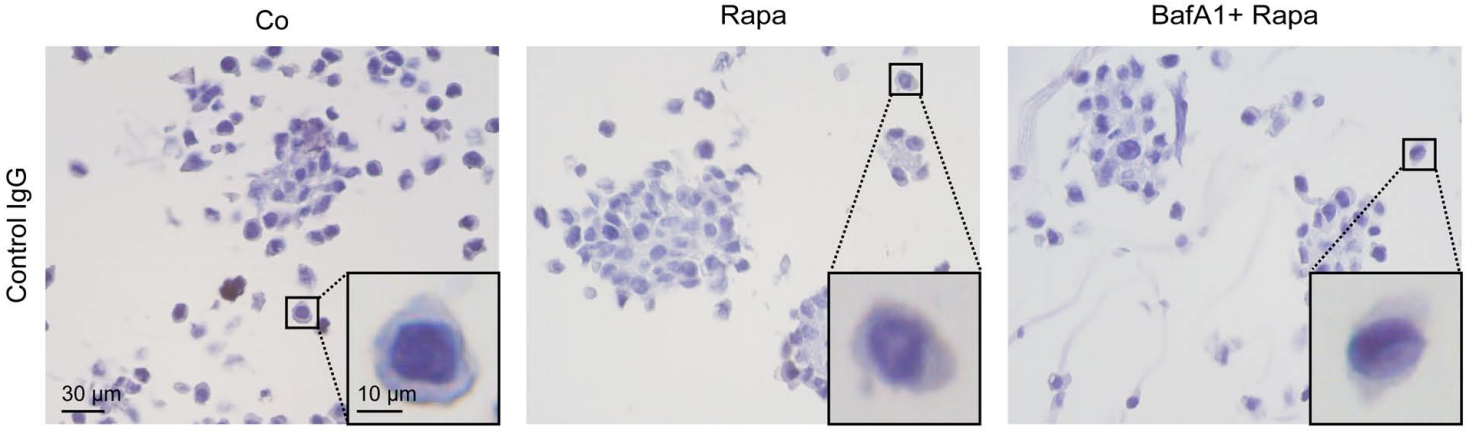

Suppl. Figure 1

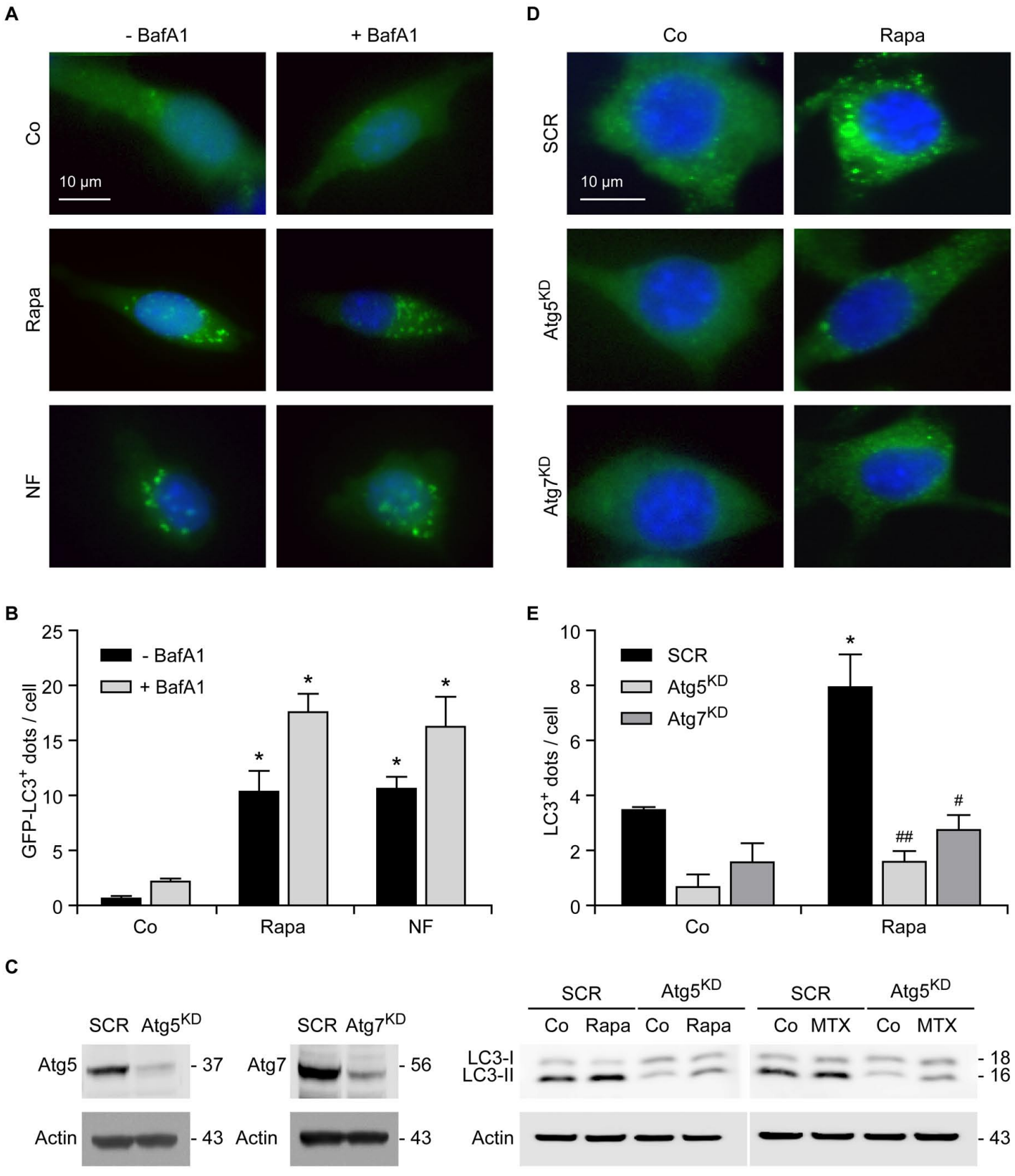

Suppl. Figure 2

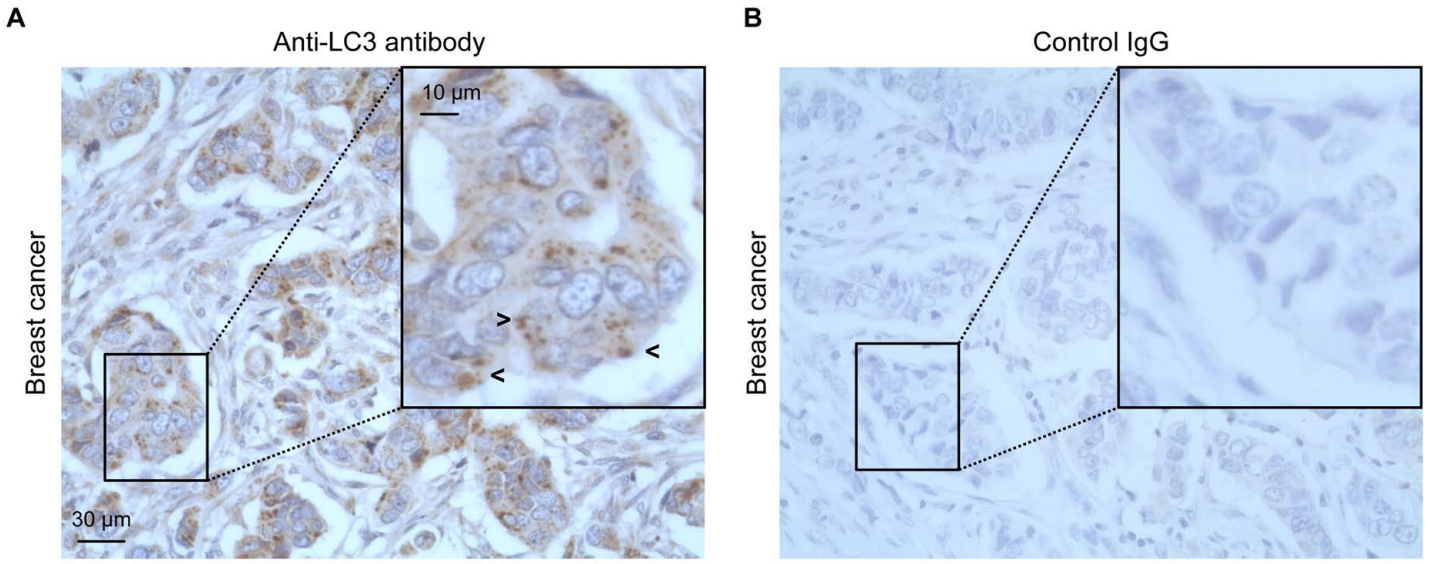

Suppl. Figure 3

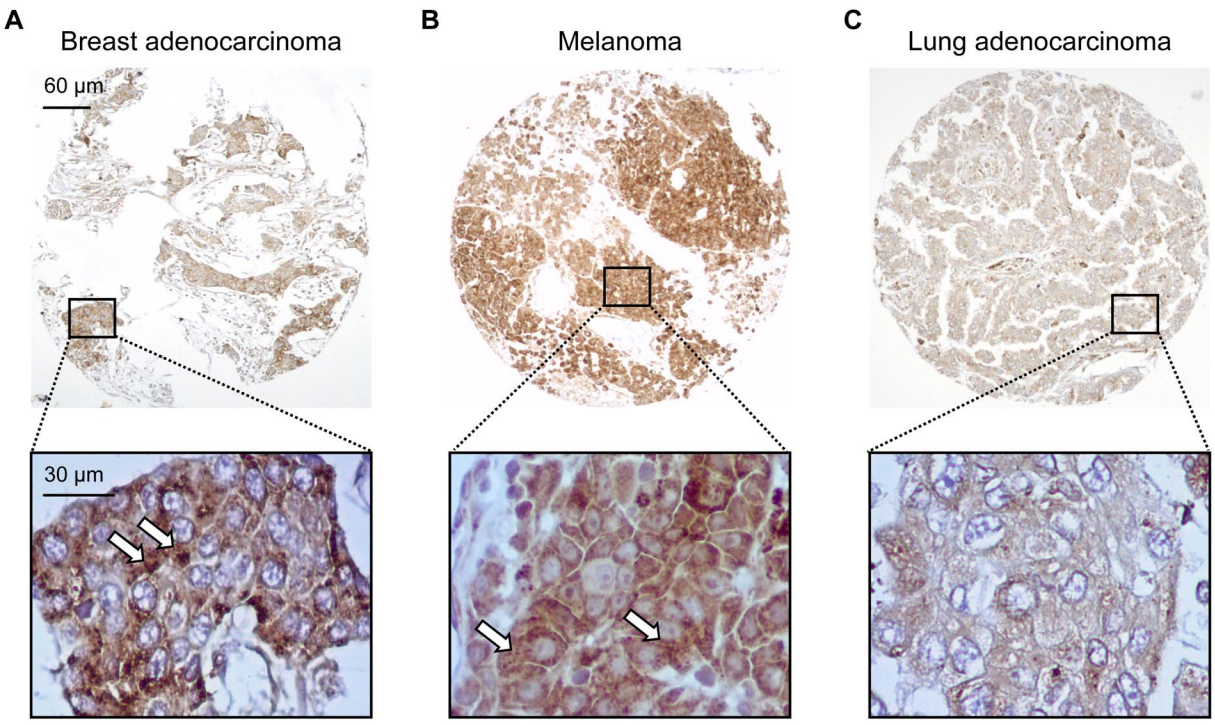

Suppl. Figure 4

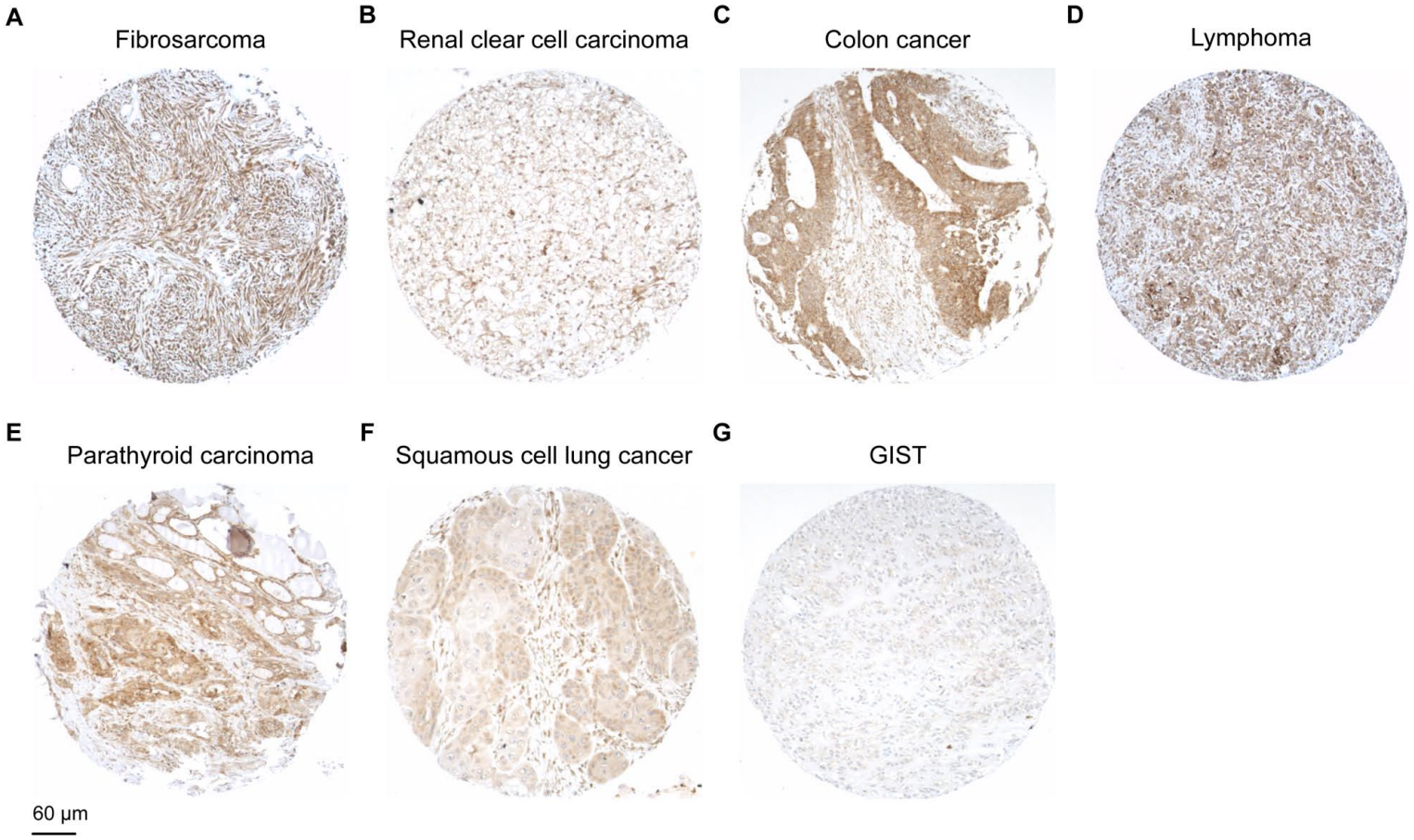

Suppl. Figure 5

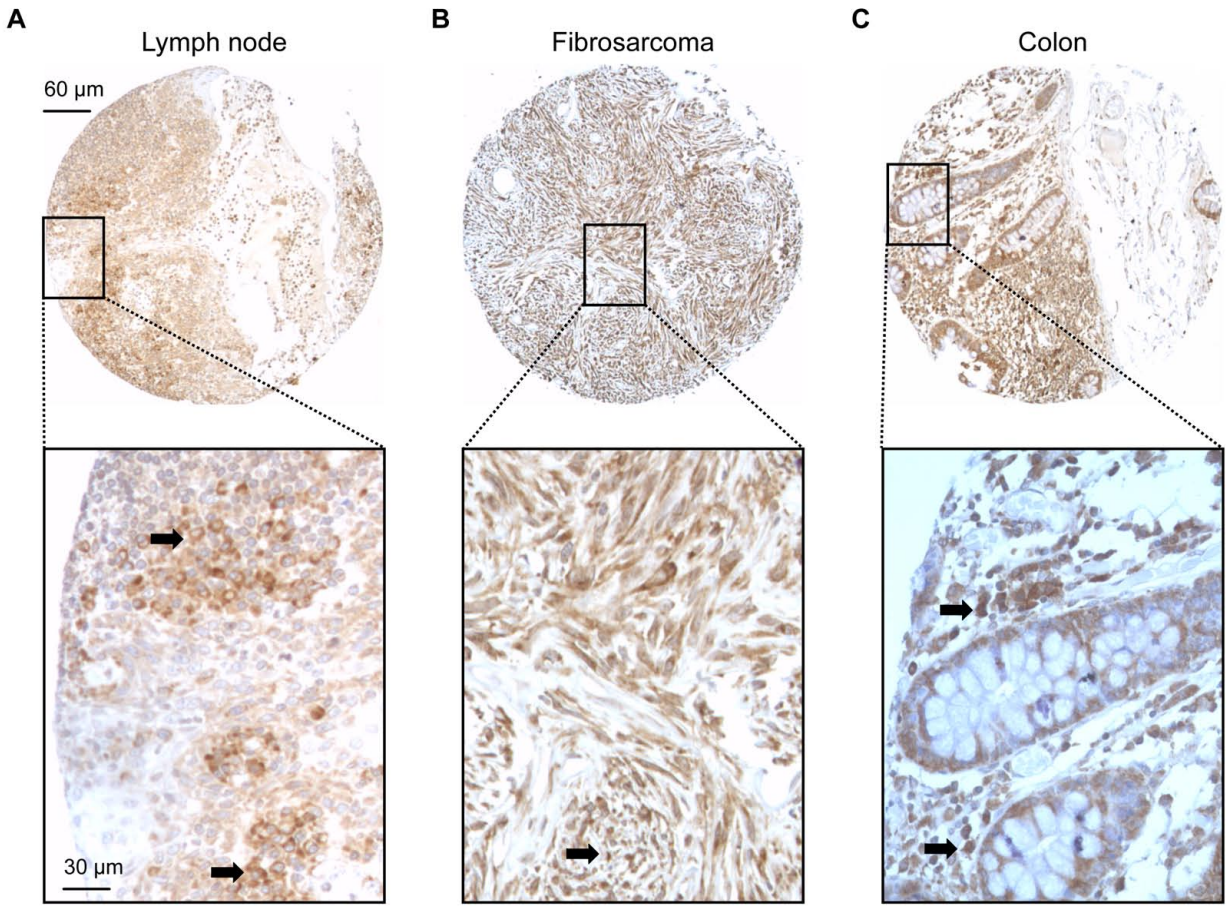

Suppl. Figure 6

Legends to Supplemental Figures

Supplemental Figure 1. **Specificity of LC3 detection by immunohistochemistry in cell pellets.** Mouse colon carcinoma CT26 cells were left untreated (Co) or treated with 10 μM rapamycin (Rapa), either in the absence or in the presence of 1 μg/mL bafilomycin A1 (BafA1), for 8 h. Thereafter, cells were processed for the immunohistochemical detection of LC3, upon replacement of the LC3-specific antibody with an isotype matched unspecific IgG. Representative images are provided. Scale bars = 10 or 30 μm, as indicated.

Supplemental Figure 2. **(Immuno)fluorescence microscopy-assisted detection of LC3 in autophagy-proficient and autophagy-deficient cancer cells. A,B**. Murine colon carcinoma CT26 cells stably expressing a GFP-LC3 fusion protein were left untreated (Co), treated with 10 μM rapamycin (Rapa) or maintained in nutrient-free (NF) conditions, in the absence or in the presence of 1 μg/mL bafilomycin A1 (BafA1) for the indicated time. Thereafter, cells were fixed and analyzed for the presence of GFP-LC3^{+} cytoplasmic dots. **C-E**. Alternatively, CT26 cells expressing a control shRNA (SCR cells) as well as cells expressing Atg5- (Atg5^{KD}) or Atg7-specific (Atg7^{KD}) shRNAs were kept in control conditions or treated with 10 μM rapamycin or 4 μM mitoxantrone (MTX) for 8 h. Thereafter, cells were processed for the immunoblotting-assisted detection of Atg5, Atg7 and LC3 (**C**), or for the immunofluorescence-based quantification of the LC3-I→LC3-II conversion (**D,E**). Representative images (**A,C,D**) and quantitative data (**B,E**) are shown. Scale bar = 10 μm. In **B** and **E**, columns report the number of GFP-LC3^{+} or LC3^{+} cytoplasmic dots/cell, respectively. Data are presented as means ± SEM (n = 3; * = p<0.05, Student's t test, compared to WT or SCR cells maintained in control conditions; # = p<0.05, ## = p<0.001, Student's t test, as compared to WT or SCR cells treated with the same autophagic trigger in

the absence of BafA1). In **C**, actin levels were monitored to ensure equal loading of lanes, and molecular weights are reported.

Supplemental Figure 3. **Specificity of LC3 detection by immunohistochemistry in human tissue sections. A,B**. Breast adenocarcinoma tissue sections were subjected to the immunohistochemical detection of LC3, either in standard conditions (**A**) or upon replacement of the LC3-specific antibody with an isotype matched unspecific IgG (**B**). Representative images are provided. Scale bars = 10 or 30 μm, as indicated. Arrowheads depict $LC3^+$ dots.

Supplemental Figure 4. **Patterns of LC3 expression in human tumors contained in tissue microarrays. A-C**. Tissue microarrays encompassing distinct neoplastic tissues were stained for the immunohistochemical detection of LC3, as detailed in Materials and Methods. Representative staining patterns are reported: LC3 puncta (white arrows) in breast adenocarcinoma (**A**) and melanoma (**B**), diffuse cytoplasmic distribution of LC3 in lung adenocarcinoma (**C**). Scale bars = 30 or 60 μm, as indicated.

Supplemental Figure 5. **LC3 staining performed on different tumor types contained in a tissue microarray. A**, fibrosarcoma; **B**, renal clear cell carcinoma; **C**, colon cancer; **D**, lymphoma; **E**, parathyroid carcinoma; **F**, squamous cell lung cancer; **G**, gastrointestinal stromal tumor (GIST). Scale bars = 60 μm.

Supplemental Figure 6 **LC3 staining of immune cells. A**. Strongly LC3-positive immune cells (black arrows) in a normal lymph node. **B**. Stromal immune cells (black arrow) in the proximity of fibrosarcoma cells. **C**. Immune cells (black arrows) close to non-malignant colon epithelial cells. Scale bars = 30 or 60 μm, as indicated.

Supplemental Table 1. **LC3 staining patterns of 49 different samples included in a tissue microarray.**

Tissue Origin	Diffuse weak cytoplasmic	Diffuse strong cytoplasmic	Diffuse strong cytoplasmic + puncta
Malignant tissues			
Breast adenocarcinoma 1			
Breast adenocarcinoma 2			**40%**
Breast adenocarcinoma 3			
Colon adenocarcinoma			**50%**
Fibrosarcoma			**80%**
GIST			
Glioblastoma 1			
Glioblastoma 2			**30%**
Glioblastoma 3			**50%**
Hepatocellular carcinoma			**100%**
Lung adenocarcinoma 1			
Lung adenocarcinoma 2			**50%**
Lung adenocarcinoma 3			
Lung squamous cell carcinoma			
Lymphoma			**50%**
Medulloblastoma 1			**100%**
Medulloblastoma 2			
Medulloblastoma 3			**80%**
Melanoma			**90%**
Meningioma 1			
Meningioma 2			
Meningioma 3			
Oligodendroglioma 1			**50%**
Oligodendroglioma 2			**30%**
Oligodendroglioma 3			
Parathyroid carcinoma 1			
Parathyroid carcinoma 2			
Parathyroid carcinoma 3			**30%**
Prostate adenocarcinoma			
Renal clear cell carcinoma			
Testicular seminoma			

Normal tissues		
Cerebellum 1		
Cerebellum 2		
Cerebral cortex		**30%**
Cerebral cortex		**30%**
Cerebral white matter 1		
Cerebral white matter 2		
Colon		
Hippocampus 1		
Hippocampus 2		**50%**
Kidney		
Liver 1		
Liver 2		
Liver 3		
Lung		
Lymph node 1		
Lymph node 2		
Placenta		
Skin		
Thyroid		

The % of cells exhibiting $LC3^{+}$ cytoplasmic dots is reported.